Article

Açaí (*Euterpe oleracea* Mart.) seed oil exerts a cytotoxic role over colorectal cancer cells: insights of Annexin A2 regulation and molecular modeling

Marcos Antonio Custódio Neto da Silva[1,2], Josiane Weber Tessmann[3], Kátia Regina Assunção Borges[2], Laís Araújo Souza Wolff[2], Fernanda Diniz Botelho[4], Leandro Alegria Vieira[4], Jose Andrés Morgado-Diaz[4], Tanos Celmar Costa França[4,5], Maria do Carmo Lacerda Barbosa[2], Maria do Desterro Soares Brandão Nascimento[2], Murilo Ramos Rocha[3,*] and João Ernesto de Carvalho[6,*]

a Faculty of Medical Science, Post-graduation in Internal Medicine, State University of Campinas, Campinas, São Paulo, Brazil (M.A.C.N.S: marcos.antonio@ufma.br)
b Nucleum of Basic and Applied Immunology, Pathology Department, Federal University of Maranhão, São Luís, Maranhão, Brazil (M.A.C.N.S: marcos.antonio@ufma.br; K.R.A.B: kareborges@gmail.com; L.A.S.W: laiswolff19@gmail.com; M.C.L.B: carminha13032009@hotmail.com; M.D.S.B.N: m.desterro.soares@@gmail.com)
c Cell Structure and Dynamics Group, Cellular and Molecular Oncobiology Program, National Cancer Institute, Rio de Janeiro, Brazil (J.W.T: josiwt@hotmail.com; J.A.M.D; jmorgado@inca.gov.br; M.R.R: rochamr.2@gmail.com)
d Laboratory of Molecular Modeling Applied to Chemical and Biological Defense (LMCBD), Military Institute of Engineering, Rio de Janeiro, Brazil. (F.D.B: fernandinhabotelho@gmail.com; L.A.V: leandrovieira@ime.eb.br; T.C.C.F: tanosfranca@gmail.com)
e Department of Chemistry, Faculty of Science, University of Hradec Kralove, Rokitansheho 62, Kralove, Czech Republic (T.C.C.F: tanosfranca@gmail.com)
f Faculty of Pharmaceutical Sciences, Post-graduation in Internal Medicine, State University of Campinas, Campinas, São Paulo, Brazil (J.E.C: carvalho@fcf.unicamp.br
* Correspondence: author: J.E.C. Rua Candido Portinari, 200 - Cidade Universitária, Campinas - SP, 13083-871. carvalho@fcf.unicamp.br. + 55 13 3521-8123 and M. R. R. Rua André Cavalcanti, 37 - Centro, Rio de Janeiro - RJ, 20231-050. rochamr.2@gmail.com. + 55 21 3207-6513

Abstract: Açaí, *Euterpe oleracea* Mart. is a native plant from the Amazonian and is rich in several phytochemicals with anti-tumor activities. The aim was to analyze the effects of açaí seed oil on colorectal adenocarcinoma (ADC) cells. *In vitro* analyses were performed on CACO-2, HCT-116, and HT-29 cell lines. The strains were treated with açaí seed oil for 24, 48, and 72 h, and cell viability, death, and morphology were analyzed. Molecular docking was performed to evaluate the interaction between the major compounds in açaí seed oil and Annexin A2. The viability assay showed the cytotoxic effect of the oil in colorectal adenocarcinoma cells. Acai seed oil induced increased apoptosis in CACO-2 and HCT-116 cells and interfered with the cell cycle. Western blotting showed increased expression of LC3-B, suggestive of autophagy, and annexin A2, an apoptosis regulatory protein. Molecular docking confirmed the interaction of major fatty acids with annexin A2, suggesting a role of açaí seed oil in modulating annexin A2 expression in these cancer cell lines. Our results suggest the antitumor potential of açaí seed oil in colorectal adenocarcinoma cells and contribute to the development of an active drug from a known natural product.

Keywords: *Euterpe oleracea* Mart; Polyphenols; Apoptosis; Autophagy; Annexin A2

1. Introduction

Cancer is a growing health problem worldwide owing to the increase in life expectancy, urbanization, and subsequent changes in environmental conditions. According to data from GLOBOCAN for 2020, 19.3 million cases of cancer and approximately 10 million deaths were estimated. The most frequent types of cancer were breast cancer (11.7%), lung

 doi:10.20944/preprints202305.1351.v1

cancer (11.4%), and colorectal cancer (10.0%). Lung cancer remains the leading cause of death from neoplasia, followed by colorectal cancer and hepatocarcinoma [1].

In Brazil, estimations for each year of the triennium 2023-2025 indicate that there will be 704,000 new cases of cancer. Non-melanoma skin cancer is the most frequent (220,000), followed by cancers of the breast and prostate (74,000 and 72,000, respectively), colon and rectum (46,000), lung (32,000), and stomach (21,000) [2].

Two of the major challenges in treating neoplasias are the inherent toxicity and side effects of anti-tumoral drugs and the development of resistance to these treatments. Hence, there is a constant search for adjuvant treatments that might increase the efficacy of traditional chemotherapeutic drugs and hinder the development of resistance. The immense biodiversity present in the Amazon Forest and the popular knowledge of its inhabitants provide fertile grounds for the discovery of new and promising neoadjuvant agents.

Açaí is considered a food of high caloric and nutritional value, with a high percentage of lipids, proteins, and minerals, and is the main food base of the riverside population of the Amazon River Estuary region [3]. Previous phytochemical analyses have revealed the presence of flavonoids, anthocyanins, benzenoid lignans, benzoquinone, monoterpenoids, norisoprenoids, and essential fatty acids [4-7]. Mantovani et al. (2003) described the predominance of unsaturated fatty acids, especially oleic acid and palmitoleic acid [8].

"Açaí" is a term from *tupi* origin "yasa'y" (i), which means "water palm tree" [9,10]. The fruits of the açaí tree are extracted wine, pulp, or simply açaí, as is known in the region. Açaí is usually eaten with *mandioca* flour, which is associated with fish, shrimp, or beef, and is the basic food for riparian communities.

In addition to serving as a food, açaí is widely used in folk medicine [11,12]. In ethnomedicine, the root and stem of leaves are used for muscular pain and snake bites, and to relieve chest pain [13,14]. The root can also be used for the treatment of malaria and liver and kidney infections [15,16]. The seed provides a dark green oil, popularly used as an antidiarrheal [15]. In 2002, a study using *Euterpe oleracea* leaves reported a reduction in abdominal contortions and peripheral analgesic action [17].

Some comprehensive studies have shown different biological activities of açaí, such as anti-lipidemic, neuroprotective, hypocholesterolemic, therapeutic, anti-inflammatory, and anti-cancer properties [18-22].

Regarding açaí oil, Melhorança Filho and Pereira (2012) and Magalhães et al. (2020) described antibacterial activity [23,24], Favacho et al. (2011) anti-inflammatory and antinociceptive effects [25], and Souza et al. (2017) antilipemic action [26].

Marques *et al* (2017) studied the açaí oil and different human cells, evaluating the cytotoxicity, genotoxicity, and antigenotoxicity of *Euterpe oleracea*. HepG2 cells (hepatoma cells) and human leukocytes were used in this study. No cytotoxic effects of the extracts were observed on the strains used [27].

Regarding its antitumoral effect, Despite the bioactive potential of açaí, only a few studies have been described in the literature, with promising results, showing the chemopreventive and therapeutic effects of açaí in different cancer models, including esophageal cancer [28], urothelial cancer [29], colon cancer [30-33], melanoma [34], and breast cancer [35-38].

Annexin A2 protein has been investigated as a prognostic marker because of its wide presentation in various forms of cancer. Deletion of the Annexin A2 gene (ANXA2) has been shown to decrease DNA synthesis and cell proliferation, suggesting that Annexin A2 is a factor in cell division [39].

Based on the current knowledge about the use of natural products with antioxidant, anti-inflammatory, and antitumor properties, our goal was to analyze the effects of açaí seed extract and oil (*Euterpe oleracea* Mart.) in different cell lines of human colon adenocarcinoma, providing evidence that suggests its use in a neoadjuvant setting after preclinical studies.

2. Materials and Methods

Preprints (www.preprints.org) | NOT PEER-REVIEWED | Posted: 18 May 2023 doi:10.20944/preprints202305.1351.v1

2.1. Materials

The following antibodies were purchased from commercial sources: anti-Bax (Cell Signaling Technology, Inc.), Anti-Bcl-2 (Cell Signaling Technology, Inc.), total Anti-Annexin A2 (Invitrogen), phospho-anti-annexin A2 (R&D Systems), and anti-LC3B (Cell Signaling Technology).

2.2. Preparation of lyophilized hydroalcoholic seed extract and oil of Euterpe oleracea Mart

The fruits of açaí (*Euterpe oleracea* Mart.) used in this study were obtained from Juçara Park (São Luís, Maranhão, Brazil). A sample of the specimen was stored under exsiccate number 30 issued by the Rosa Mochel Herbarium of the Nucleus of Biological Studies of the State University of Maranhão (UEMA), and deposited with the World International Property Organization under registration number PI0418614-1.

The fruits were previously refrigerated at -20 °C in the Laboratory of Cell Culture of the Nucleus of Basic and Applied Immunology of the Federal University of Maranhão (UFMA). After thawing at room temperature, the samples were separated into three parts: the seed, pulp, and total fruit (seed + pulp). The extraction process followed the methodology developed by de Moura *et al.* (2012) [40].

Approximately 360 g of açaí was washed with tap water and boiled in distilled water for 5–10 min. Subsequently, the portions were ground and homogenized with 400 ml of ethanol under stirring for 2 h. The resulting extracts were stored at 4°C protected from light for 10 d. After this maturation period, the hydroalcoholic extracts were filtered through Whatman # 1 filter paper, and the liquid phase concentrated in a low pressure rotary evaporator (Fisatom Equipamentos Científicos Ltda., São Paulo, Brazil) at approximately 40 °C and then lyophilized (LIOTOP model 202, Fisatom Equipamentos Científicos Ltda., São Paulo, Brazil) at a temperature of -30 to -40 ºC and a vacuum of 200 mm Hg. The extracts were kept at -20 ° C until the day of use.

For oil extraction, the fruits were washed under running water and subsequently subjected to pulping. After this process, 360 g of crushed seeds of *Euterpe oleracea* Mart was dried in the sun and crushed in a mill. After the afore mentioned pre-treatment, the oil was extracted using a Soxhlet extractor. The solvent used in the process was n-hexane and the total extraction time was 6 h.

2.3. MS/MS analysis

Crude extracts of the seeds, pulp, and total fruit of açaí (*Euterpe oleracea* Mart) were suspended in 2 ml of MeOH HPLC and centrifuged at 13000 rpm for 5 min. The supernatant solution (100 µL) was filtered through a 0.22 µm and diluted into 900 µL MeOH HPLC. The samples were analyzed using an LC Agilent 1200 mass spectrometer coupled with an Agilent iFunnel 6550 Q-ToF LC/MS. The electrospray ionization source operated in positive mode ESI (+), following operating conditions: nebulizing gas temperature, 290 °C; capillary voltage, +3500 V; nozzle voltage, 320 V; drying gas flow, 12 ml min−1; nebulization gas pressure, 50 psig; auxiliary gas temperature, 350 °C; and flow of auxiliary gas: 12 ml min^{-1}. The analyzer time-of-flight (ToF) was operated in the range *m*/*z* 50–1500. Collision Energy formula (auto MS/MS mode):4 V (slope) × (*m*/*z*)/100 + 5 V (offset). A maximum of five precursors per cycle were selected. Stationary phase: Thermo Scientific Accucore C18 2.6 µm, 2.1 mm x 100 mm). Mobile phase: acetonitrile and 0.1% formic acid. Flow rate:0.2 mL min^{-1}. The organic phase was run in gradient mode from 5% to 98% within 10 min, held for 5 min, up to 5% within 1.2 min and hold for 4.8 min. Total run time: 20 min. The injection volume used was2 µL. The spectra were processed using Agilent Mass Hunter Workstation Software.

2.4. Oil esterification

The crude oil of *Euterpe oleracea* Mart was analyzed in the form of methyl esters prepared according to Hartman and Lago (1973) [41]. The oil (100 mg) was weighed and placed in 20 mL tubes with a screw cap. Then, 4 mL of a 0.5 mol/L solution of sodium

 doi:10.20944/preprints202305.1351.v1

hydroxide in methanol was added. The mixture was heated for a period of 5 min in a boiling water bath until the fat globules completely dissolved, and the tubes were quickly cooled in running water, immediately adding 5 mL of a solution previously prepared with 1 g of ammonium chloride, dissolved in 30 ml of methanol and 1.5 ml of sulfuric acid, concentrated in small portions, with stirring. Afterwards, the tube was shaken, heated in a boiling water bath for 5 min, cooled under running water, and 4 mL of saturated sodium chloride solution was added and stirred for 30 s. Finally, 5 ml of hexane was added, and the tube was shaken vigorously using a vortex mixer for 30 s and left to rest for complete separation of the phases, which were kept cooled for chromatographic analysis.

2.5. GC-MS analysis

Fatty acid identification was performed using a gas chromatograph (GC-2010) coupled to a mass spectrometer (GC-EM QP2010 Plus; Shimadzu). For chromatographic analysis, a capillary column ZB-FFAP (30m x 0.25 mm x 0.25µm) was used for the chromatographic analysis. The flow of carrier gas was helium at a linear speed of 30 cm/s and column flow of 1.0 ml / min. The oven program was: 120 °C for 2 min with a heating ramp of 10 °C/min up to 180 °C that remained for 5 min, being heated again at a rate of 5 °C/min up to 230 °C, remaining for to 25min. The temperatures of the injector and the ion source were 200 °C and 250 °C, respectively. Split injection mode at a ratio of 50.

The quantification of fatty acids was performed by normalizing the peak areas, and the identification of esters from the fatty acids that make up the oil was performed using the NIST08 equipment library (National Institute of Standards and Technology).

2.6. Cell culture

Human colorectal adenocarcinoma cell lines HT-29 (HTB-38TM), HCT-116 (ATCC® CCL-247™), and Caco-2 (HTB-37TM) were obtained from the American Type Culture Collection (Manassas, VA, USA). The cells were grown in Dulbecco's modified Eagle's medium (Invitrogen Inc.) supplemented with 10% fetal bovine serum (FBS), penicillin G (60 mg/L), and streptomycin (100 mg/L) at 37 °C in a humidified atmosphere of 5% CO_2/air, and the cells were passaged weekly by using a solution of 0.05% trypsin/0.02% EDTA in PBS. For experiments, cells were seeded into culture flasks, plates, or glass coverslips.

2.7. Treatments with Euterpe oleracea Mart seed extract and oil

Samples were diluted in dimethyl sulfoxide (DMSO) stock solutions (Merck) at a concentration of 0.1g/mL. Cells were seeded in 96-well plates at a concentration of ($1x10^4$ cells/mL) and after 24h were treated with 0.25, 2.5, 25, or 100 µg/mL açaí seed extract and oil. The cell viability was assessed at 24, 48, and 72 h.

2.8. Cell Viability Test - MTT

Cells were trypsinized and counted in a Neubauer chamber, and an aliquot of 1×10^4 cells/ml was cultured in 96-well plates in the presence or absence of the extract and oil. After 24 and 48 h of treatment, 200 µl of fresh medium containing 10 µl of 3-(4,5-Dimethylthiazol-2-yl)-2,5-diphenyltetrazolium bromide (MTT) was added to the culture. The cells were re-incubated in a CO_2 incubator for 3 h, protected from light. Subsequently, The plates were centrifuged at 1200 rpm for 5 min at 4°C. The supernatant was discarded, and 100 µl of (dimeyl sulfoxide DMSO () was added to each well. The absorbance was measured on a Spectra Max 190 plate spectrophotometer (Molecular Devices, Sunnyvale, CA, USA) at a wavelength of 538 nm.

In view of the initial results and to evaluate the mechanism of action of açaí seed oil, CACO-2, HCT-116, and HT-29 cells were pre-treated with N-acetylcysteine (NAc), a known antioxidant, at doses of 2.5, 5 and 10mM for 2h before treatment with açaí seed oil at concentrations of 25 and 50 µg/mL for 24h. Cells were quantified using Trypan blue to

 doi:10.20944/preprints202305.1351.v1

assess the percentage of viable cells, and then a cell viability assay was performed using MTT.

2.9. Morphological analysis by inverted light microscopy

Cell morphology was analyzed by light microscopy after treatment with açaí seed extract, and oil was analyzed using an inverted Axio Observer Z1 microscope equipped with an Axiocam HRc Ver.3 chamber. Image analysis was performed using Axiovision Release 4.8.1 software (Carl Zeiss Inc., Germany). The cells were cultured in 12-well plates in the presence or absence of açaí seed oil for 24 and 48 h and then observed under a microscope.

2.10. Annexin – V assay

After a 24h incubation period, the cell suspensions were centrifuged at 1000 rpm (168 g) for 10 min and resuspended in PBS (pH 7.4). Then, the cells were centrifuged again at 1000 rpm (168 × g) for 10 min.

Subsequently, viable, apoptotic, and nonviable cells were determined using an ANNEXIN V-FITC apoptosis detection kit containing annexin V-FITC, propidium iodide, and buffer (BD Biosciences).

After the second centrifugation, the cells were resuspended in binding buffer previously diluted in deionized water at a ratio of 1:10. Then, 500 µL of the cell suspension was labeled with 5 µL annexin V-FITC and 10 µL propidium iodide.

After 10 min of rest in the dark, cell fluorescence was immediately determined using a flow cytometer. Cells in the early stages of apoptosis were marked intensely by annexin V-FITC, which emits green fluorescence as a result of its preferential binding to phosphatidylserine residues, externalized at the beginning of the process. Necrotic or non-viable cells were marked intensely by propidium iodide, which emits red fluorescence, and less intensely by annexin V-FITC. Viable cells were not labeled with annexin V-FITC or propidium iodide.

Excitation was performed using an argon laser operating at 488 nm and fluorescence detection was performed at 530 nm (PI) and 670 nm (7-AAD).

2.11. Western Blotting

Western blotting was performed as described by Albuquerque-Xavier et al. (2012) [42]. The cells were treated for 12 h with açaí seed oil and the protein content was extracted. Total cell lysate will be obtained by incubating cells with lysis buffer (1% Triton X-100, 0.5% sodium deoxycholate, 0.2% SDS, 150mM NaCl, 2mM EDTA, 10mM HEPES (pH 7.4) containing 20mM NaF, 1mM orthovanadate and protease inhibitor cocktail (1:100 dilution) for 30 min at 4°C, and centrifuged at 10,000 g for 10 min at 4°C. The supernatant will be removed and stored at -20°C until further use.

Protein quantification was performed using the BCA kit (Bio-Rad, Hercules, CA, USA). Proteins (40µg/ml) were electrophoretically separated by SDS-PAGE on 13% gels and transferred to a nitrocellulose membrane (Bio-Rad) for 1h at 10V. After blocking with 5% milk for 1 h, the membrane was incubated overnight at 4°C with anti-LC3B antibody (1:1500), anti-Bax (1:250), Anti-Bcl-2 (1:1500), total and phosphorylated anti-annexin A2 (1:1400). Subsequently, the membrane was washed with TBS-T buffer (20 mM Tris-HCl pH 7.6, 137 mM NaCl, and 0.1% Tween-20) and incubated for 1 h with HRP-conjugated anti-rabbit IgG secondary antibody (1:10000).

The proteins were visualized using a chemiluminescence kit (Amersham Biosciences, Buckinghamshire, UK). All membranes were reused for GADPH labeling to confirm the application of the same amount of protein in all wells. The intensity of the bands was quantified according to their thickness using LabWorks 4.6 program (Bio-Rad Laboratories, Hercules, CA).

2.12. Molecular modeling studies

 doi:10.20944/preprints202305.1351.v1

2.12.1. Obtention of the 3D structure of annexin A2 and construction of the ligands

The 3D structure of annexin A2 (ANXA2) in complex with a tetrasaccharide derived from heparin was downloaded from the Protein Data Bank website (www.rcsb.org) under the PDB ID:2HYU [43]. This structure was used for modeling ANXA2 interactions with the five most abundant fatty acids in the extract.

The 3D structures of the five fatty acids investigated in this work (palmitic, myristic, lauric, oleic, and linoleic) were constructed using software Spartan 8 [44] and optimized using the semi-empirical method PM3 [45], with the atomic partial charges calculated using the Natural Population Analysis method [46]. The molecules were then transferred (together with the ANXA2 structure downloaded from the PDB (www.rcsb.org) to the Molegro Virtual Docker software (MVD®) to run the docking studies.

2.12.2. Docking studies

To verify the protein's preferential region for the docking of fatty acids, they were submitted to blind docking over a search spaced with the whole protein structure, where the best 100 poses of each ligand were collected. Subsequently, further docking runs were performed, this time with the search spaces restricted to the two regions that concentrated the larger number of poses during the blind docking. For each docking, six runs were performed, with the 30 best poses collected after each run. These poses were analyzed according to their Moldock scores and positions on the surface of the protein. The most representative positions of each ligand in both regions were selected for further MD simulation studies. The protocols used to perform all docking studies were the same as those previously validated and used [47-49].

2.12.3. Molecular dynamics simulations

The complexes between ANXA2 and the best poses obtained from the docking studies were subjected to additional MD simulations using the software GROMACS 2019.4 [50,51] and the force field OPLS/AA [53,53]. Each pose was first submitted to the Open Babel [54] and *Antechamber Python Parser Interface* (ACPYPE) [55] software to generate their coordinates (. growth extension) and topology (. top extension) files must be recognized by GROMACS 2019.4 [50,51]. The coordinate and topology files of ANXA2 were generated using the routine pdb2gmx of GROMACS 2019.4 [50,51], with further selection of the force field OPLS/AA [52,53].

Each protein-ligand complex was centered in a cubic box of 929 nm^3, with a minimal distance solute-box wall (1.5 nm) containing approximately 28,000 TIP3P [55] water molecules under periodic boundary conditions (PBC). Next, the complexes were subjected to two steps of energy minimization using the *steepest descent* algorithm, with and without position restraints (PR) of the protein and ligand, and convergence criteria of 100.00 kJ mol^{-1} nm^{-1}. After energy minimization, two equilibration steps meant to bring the system to physiologic conditions of T = 310 K and P = 1 Bar, were performed. The first step ran under constant T and V (NVT), whereas the second ran under constant T and P (NPT). The stabilities of T and P were maintained using the thermostat *Velocity-rescale* [56] and Parrinello and Rahman (1981) pressure coupling methods [57], respectively.

The production step consisted of 50 ns of free MD simulation for each system at 310 K and 1 bar, with an integration time of 2 fs, and a cut-off of 1.2 nm for VDW and electrostatic interactions. The coordinates and energy data of the complexes were stored after each 10 ps of simulation to enable further analysis of temporal properties such as total energy, root mean square deviation (RMSD), and average number of H-bonds. All analyses were performed using the software xmgrace 5.1.25 [58] and Visual Molecular Dynamics 1.9.3 (VMD) [59].

2.13. Statistical Analysis

For statistical analysis of the experimental data, one- or two-way analysis of variance (ANOVA) tests were performed, followed by Dunnett's or Tukey's post-hoc tests,

 doi:10.20944/preprints202305.1351.v1

according to the type of analysis. Differences were considered statistically significant at $p<0.05$. Statistical analysis was performed using GraphPad Prism version 8.4.0 for Windows (GraphPad Software, San Diego, CA, USA).

3. Results

3.1. Açaí seed extract is rich in flavonoids

For *Euterpe oleracea* Mart seed extract, were identified 13 compounds, especially flavonoids and anthocyanins. The major compounds were: epicatechin, kaempferol-3-O-rutinoside (Fig 1A), nobiletin, dihydrokaempferol, diosmetin, 3-O-Methylquercetin or isorhamnetin, isoorientin, 3-Genistein-8-C-glucoside and apigenin 6,8-digalactoside**.**

The yield of the oil obtained in 360g of seed was approximately 5.6%. The oil is composed of 49.3% of saturated fatty acids and 50.7% unsaturated fatty acids, 29.7% monounsaturated and 21% polyunsaturated. The major methyl esters were oleic, linoleic, myristic and palmitic acid. However, other esters appear in smaller amounts from capric, palmitoleic, linolenic, stearic, eicosanoic, behenic fatty acids and tricosanoic acid (Table 1 and Fig 1B).

Preprints (www.preprints.org) | NOT PEER-REVIEWED | Posted: 18 May 2023 doi:10.20944/preprints202305.1351.v1

Table 1. Esters from fatty acids found in Euterpe oleracea Mart seed oil

Fatty Acids	Peaks	Carbon chain	% area - Retention time (min)	Retention time (min)
Capric acid	1	C10:0	0.13	3.429
Lauric acid	2	C12:0	8.9	5.407
Myristic acid	3	C14:0	18.03	7.508
Palmitic acid	4	C16:0	16.61	9.845
Palmitoleic acid	5	C16:1	0.58	10.206
Stearic acid	6	C18:0	1.81	13.765
Oleic acid	7	C18:1	26.94	14.228
Acid (isomer)	8	C18:1	2.21	14.348
Linoleic acid	9	C18:2	19.92	15.223
Linolenic acid	10	C18:3	0.62	16.538
Nanodecenoic acid	11	C19:0	0.21	17.985
Eicosenoic acid	12	C20:0	0.35	18.326
Non-esterified myristic acid	13	C14:0	1.75	19.134
Behenic acid	14	C22:0	0.43	21.586
Eicosatrienoic acid	15	C23:0	0.22	21.904
Non-esterified palmitic acid	16	C16:0	0.88	22.649
Tricosanotrienoic acid	17	C23:0	0.22	23.212

Preprints (www.preprints.org) | NOT PEER-REVIEWED | Posted: 18 May 2023 doi:10.20944/preprints202305.1351.v1

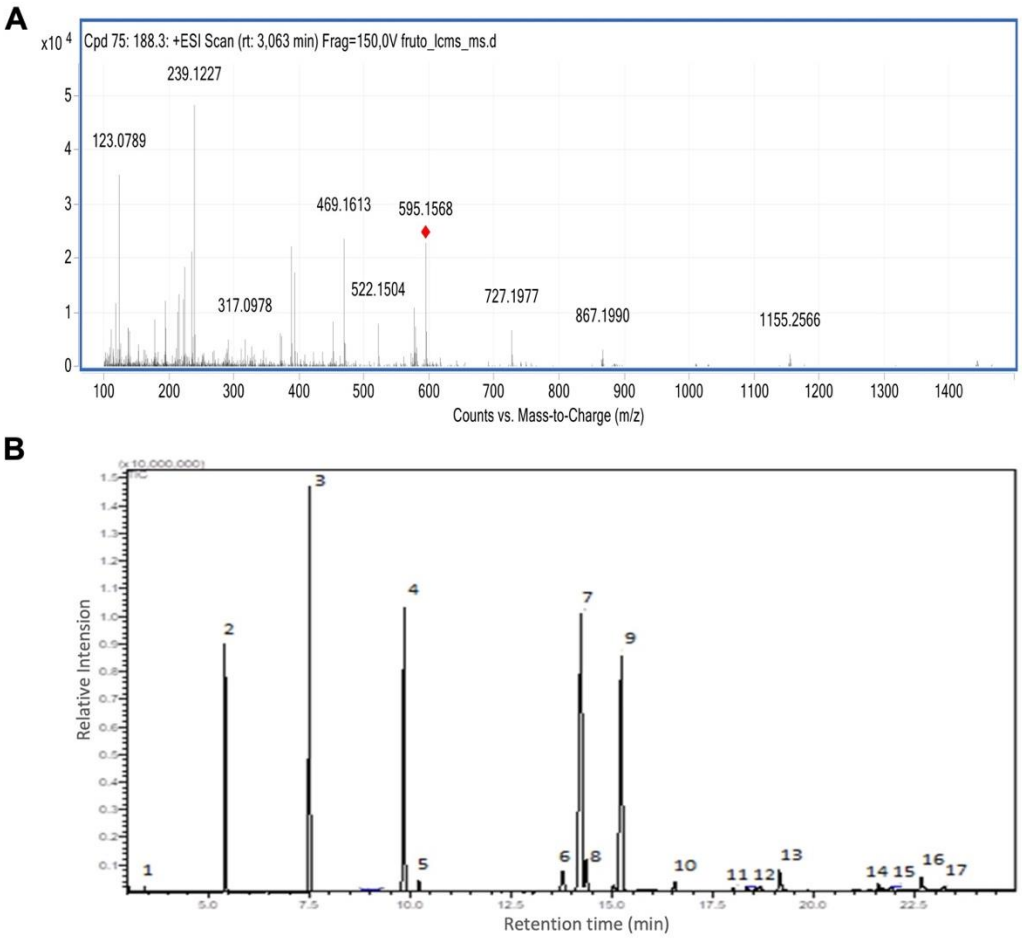

Figure 1. Açaí seed extract and oil characterization (**A**) Mass Spectrum of $[M+H]^+$ of kaempferol-3-O-rutinoside (**B**) Chromatogram of esters from fatty acids in seed oil from *Euterpe oleracea* Mart.

3.2. Açaí seed oil, but not extract, exerts cytotoxic effect in colorectal cancer cell lines

The cytotoxic effect of the of *E. oleracea* Mart. seed oil (in the concentrations 0.25, 2.5, 25 and 100 μg/mL) was analyzed by the MTT (3-(4,5-Dimethylthiazol-2-yl)-2,5-diphenyl-tetrazolium bromide) assay in three colon adenocarcinoma cell lines: Caco-2, HCT-116 and HT-29.

There was no cytotoxic effect of açaí seed extract on colorectal adenocarcinoma cell lines (Figure 2A). For the açaí seed oil there was a reduction in cell viability after 24h at concentrations of 25 and 100 μg/mL in the cell lines Caco-2 ($p<0.05$) and HCT-116 (trend). In the HT-29 cell line, there was a trend of reduction in cell viability only at the concentration of 100 μg/mL (Figure 2B). After 48h, treatment with 25 μg/mL seems not to disturb typical morphology in HT-29 cells but lead to noticeable damage and cell death in the other two cell lines (Figure 2C).

The IC50 was calculated after 24 hours of treatment with açaí seed oil. The most sensitive strain was HCT-116 with an IC50 of 11.8 μg/mL and the most resistant was HT-29 with an IC50 of 51.2 μg/mL (Figure 2D).

Preprints (www.preprints.org) | NOT PEER-REVIEWED | Posted: 18 May 2023 doi:10.20944/preprints202305.1351.v1

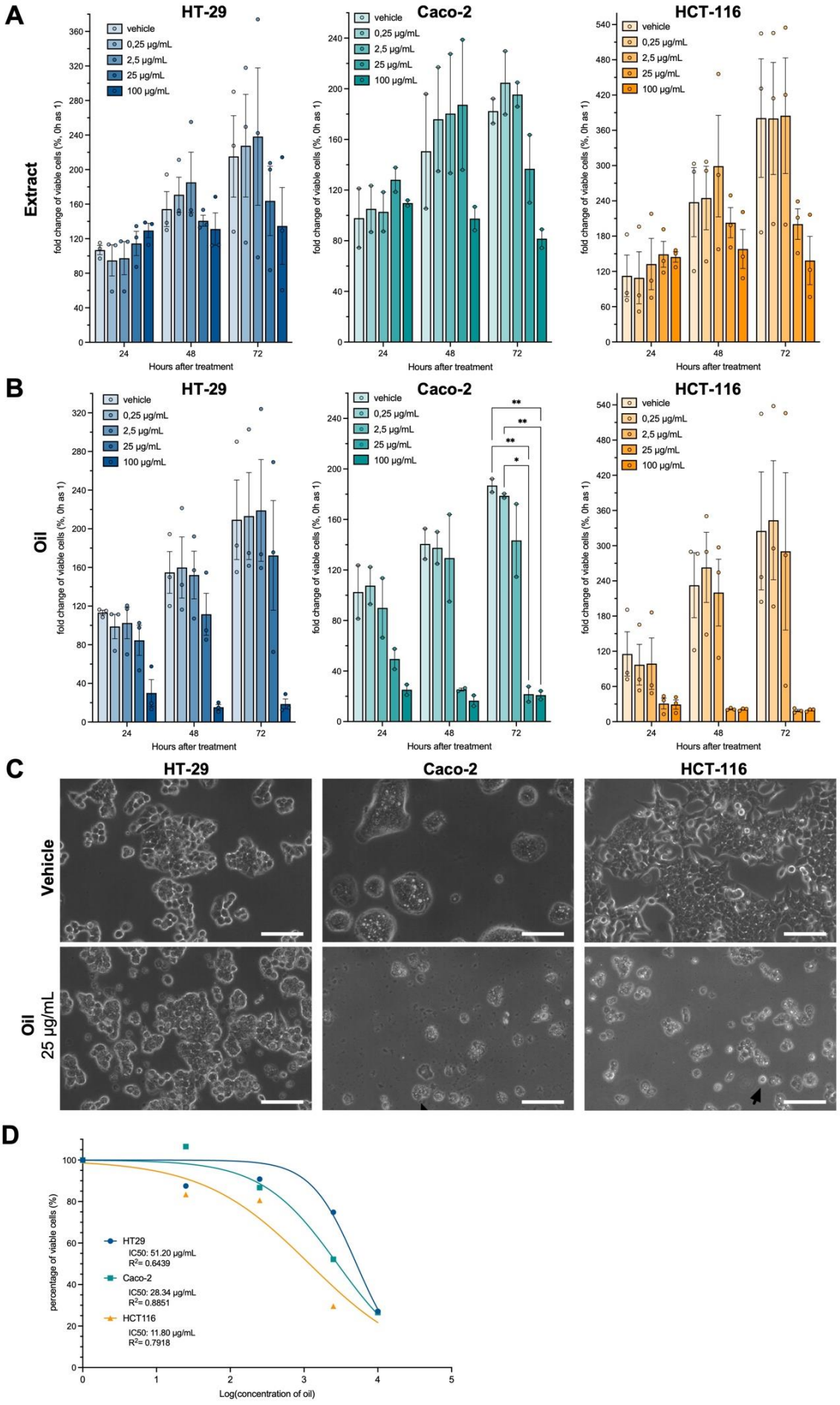

 doi:10.20944/preprints202305.1351.v1

Figure 2. Açaí seed oil is cytotoxic in a cell line-specific manner (**A**) Viability measurement in a MTT assay of three cell lines treated with açaí seed extract (**B**) Viability measurement in a MTT assay of three cell lines treated with açaí seed oil (**C**) Phase contrast micrographs of colon adenocarcinoma cell lines treated for 48h with 25ug/ml of açaí seed oil (**D**) IC50 determination for each cell line treated for 24h with açaí seed oil. Two-way ANOVA followed by Tukey posthoc. Sphericity was assessed and Greenhouse-Geiser correction used when necessary. *p<0.05; **p<0.01. Scalebar = 20 μm.

3.3. Açaí seed oil induces cellular death through increased ROS

To assess whether the reduction in cell viability occurred due to apoptotic cellular death Annexin V/PI assay was performed. Figure 3A show that treatment with 25 μg/ml of açaí seed oil increased the percentage of cells in early and late stages of apoptosis in the lines Caco-2 and HCT-116. There was no induction of apoptosis for HT-29 at the analyzed concentration.

Then, cell viability was initially evaluated with manual counting of dead and alive cells after treatment with açaí seed oil and in cells pre-treated for 2 h with 5 mM of n-acetylcysteine (NAc), to evaluate if the reduction in cell viability occurred due to an increase in free radicals.

For the Caco-2 line, cells pretreated with NAc showed a slight increase in the percentage of live cells when compared to cells treated with oil at concentrations of 25 and 100 μg/mL. In HCT-116 cells, there was an increase in cell survival when pretreated with NAc + 25 μg/mL oil. For the concentration of 100 μg/mL, there was no increase when pretreated with NAc, as this concentration is very cytotoxic for this cell line. For the HT-29 lineage, there was a significant increase in tumor cell survival when pretreated with NAc + 100 μg/mL oil (Figure 3B).

To confirm the results obtained with the quantification of dead and live cells with the Trypan blue stain, a cell viability assay was performed with MTT. All cell lines were pretreated with NAc at concentrations ranging from 2.5 to 10 mM for 2h and then treated with açaí seed oil at concentrations of 25 and 50 μg/mL for 24h.

For the Caco-2 cell line, pretreatment with NAc did not increase cell viability at the three concentrations analyzed when compared to treatment with açaí seed oil at the concentrations tested. HCT-116 cells pre-treated with 10mM NAc and exposed to 50ug of açaí seed oil exhibited an increase of cellular viability when compared to control (no pre-treatment. The same pattern was observed for HT-29 cells (Figure 3C).

Preprints (www.preprints.org) | NOT PEER-REVIEWED | Posted: 18 May 2023 doi:10.20944/preprints202305.1351.v1

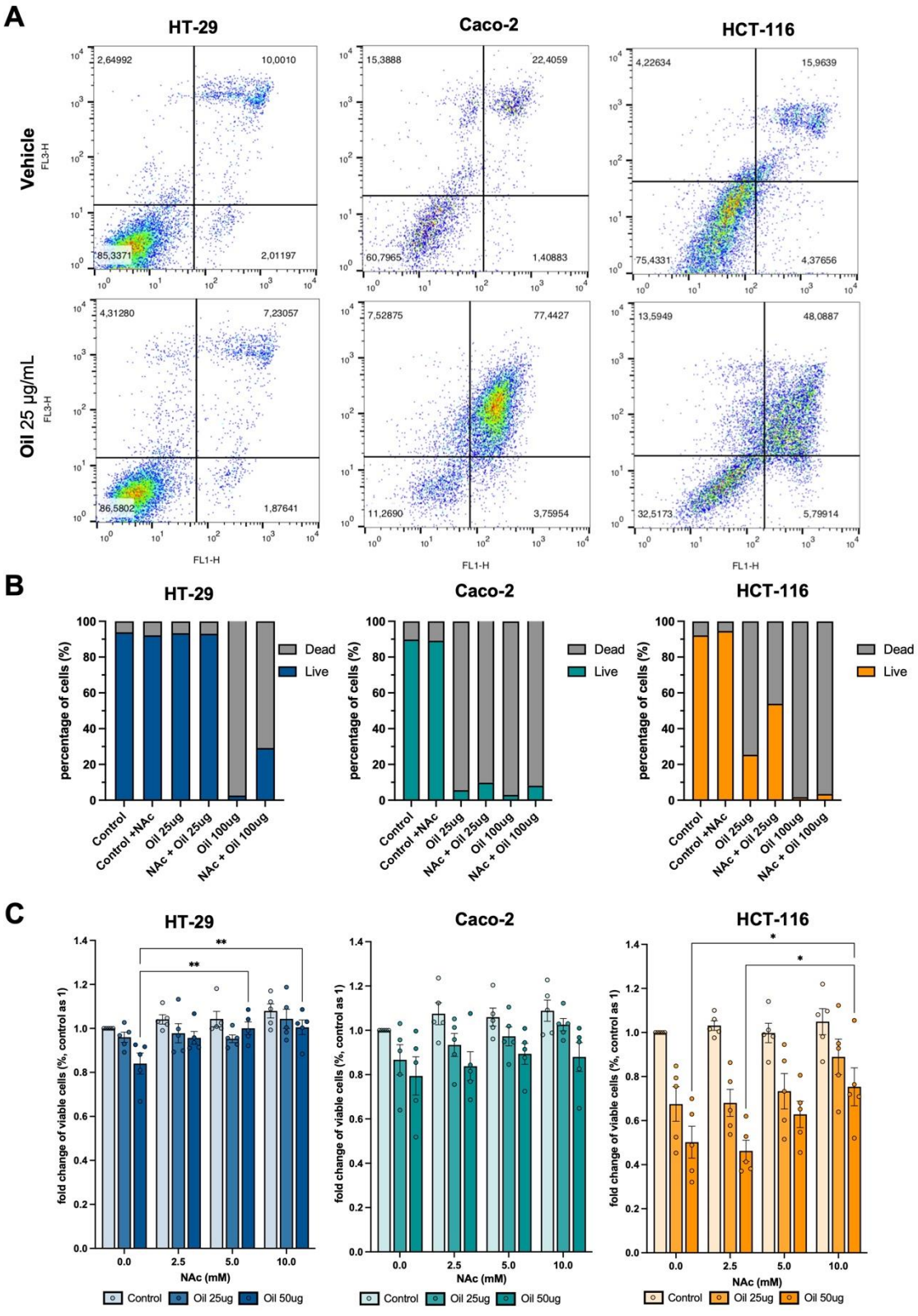

Figure 3. Açaí seed oil induces cell death which can be partially reverted through the inhibition of reactive oxygen species (**A**) Annexin V/PI assay read in the flow cytometer indicating increased apoptotic death in Caco-2 and HCT-116 cell lines 24h after 25ug/ml açaí seed oil treatment. (**B**) Trypan blue assessment of live/dead cells through manual counting of cells pre-treated with 5mM NAc for 2h and then exposed to 25 or 100ug/ml açaí seed oil. (**C**) Viability measurement in a MTT assay of three cell lines treated with açaí seed oil and a gradient of NAc (0 – 2.5 – 5 – 10) to evaluate ROS impact over oil-induced death. Two-way ANOVA followed by Tukey posthoc. Sphericity was assessed and Greenhouse-Geiser correction used when necessary. *p<0.05; **p<0.01.

Preprints (www.preprints.org) | NOT PEER-REVIEWED | Posted: 18 May 2023 doi:10.20944/preprints202305.1351.v1

3.4. Autophagy and Annexin A2 seem to participate in cellular response to açaí seed oil

Considering the role of reactive oxygen species in the death induced by açaí seed oil treatment, autophagic process was analyzed through the presence of the LC3-B II protein. During autophagy, LC3B-I protein is converted into LC3B-II, and therefore the ratio LC3BII/LC3B-I is related to an increase of autophagosome formation [60]. Annexins are a family of calcium-dependent phospholipid-binding proteins involved in membrane trafficking and organization. Annexin A2 (ANXA2), one of the twelve human annexins, has been linked to a variety of tumors including colorectal cancer (CRC). Due to its phospholipid binding properties and relation to autophagy and oxidative stress, ANXA2 level was also assessed with Western Blotting.

The protocol for this analysis was comprised of a 5mM NAc 2 hour pre-treatment and then incubation with 25ug/ml açaí seed oil in culture media with its respectives controls for the three cell lines. An decrease in LC3B-II/LC3B-I protein level was observed in Caco-2 and in greater magnitude in HCT-116 cells when compared to HT-29. This might explain their enhanced sensitivity to ROS-mediated cytotoxic effects of the açaí seed oil. Annexin A2 levels go in the opposite direction with higher values of its heavier isoform in HCT-116. It is interesting to observe that the lighter bands are indicative of apoptosis. The cell cleaves ANXA2 forming a truncated shape when apoptotic process is undergoing. These bands were seen in Caco-2 and more intense in HCT116 which corroborates previous results. Also the pretreatment shows a reduction in this truncated form, confirming their effectiveness in preventing ROS-mediated apoptotic induction from açaí seed oil treatment (Figure 4).

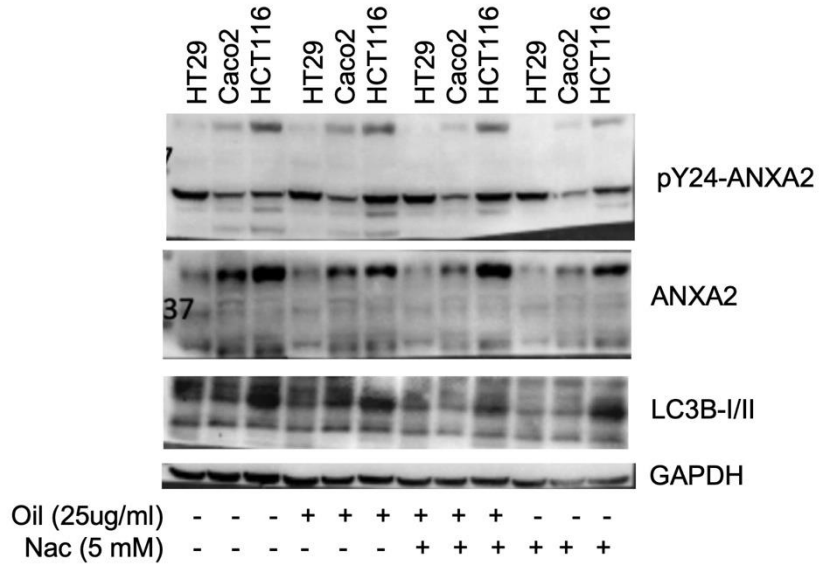

Figure 4. LC3B and ANXA2 protein levels are related to ROS-mediated apoptosis after açaí seed oil treatment. Analysis of total and Y24-phosphorylated ANXA2 and LC3B protein through Western Blotting. Cells were pre-treated with 5mM of NAc and treated with 25ug/ml (with their respective controls). GAPDH was used as housekeeping.

3.5. Docking

The search space involving the whole ANXA2 structure used for the first docking run consisted on a sphere with radio = 46 Å centered at coordinates x = -11.99; y = 1.01 e z = 214.91. This run showed that most of the poses of the five fatty acids concentrated in the same two regions of ANXA2 circled in Figure 5A. Those regions were, therefore, defined as the preferential binding regions of those molecules over ANAX2 and two new search spaces were, then, defined over them, both consisting of spheres with radio = 20 Å but coordinates centered, respectively, at coordinates x = -10,04; y = -7,17 e z = 224,46 (region 1 in Figure 5A) and: x = -5,62; y = -14,21 e z = 198,75 (region 2 in Figure 5A). It's important

Preprints (www.preprints.org) | NOT PEER-REVIEWED | Posted: 18 May 2023 doi:10.20944/preprints202305.1351.v1

to notice that region 2 is also where the protein S100A10 binds to ANXA2, forming an heterotetrametric complex containing two units of ANXA2 and two units of S100A10 [60]. There are some literature reports arguing that this tetramer might have an important role in the development and multiplication of cancer cells [61-63]. Therefore, the binding of the fatty acids to this region might avoid the formation of the tetramer, consequently, reducing the rate of multiplication of cancer cells.

As mentioned in the methodology, one pose of each fatty acid on each region circled in Figure 5, was selected for additional steps of MD simulation. The poses chosen were the ones showing the lowest Moldock score, besides being representative of that ligand, i.e having many other similar poses in that region from the blind docking. This suggests a higher probability of the ligand adopting that conformation after complexing with ANXA2. The energy values obtained for the selected poses, as well as the residues observed forming H-bonds during the docking runs, are listed in Table 2, while the respective poses are illustrated in Figure 5B. In Table 2 it's possible to see that all poses show negative energy values, ranging from -84.00 to -112 Kcal.mol^{-1}. This suggests that the fatty acids have a good affinity for ANXA2 and are capable of complexing in regions 1 and 2.

It's important to notice that the two poses selected for the myristic acid are very similar and fall both in the interface between regions 1 and 2. The difference observed between them is the fact that in one case the carboxyl group is inside the protein, while in the other it's pointing outside.

Table 2. Energy values and interaction residues of the fatty acids in the regions 1 and 2 of ANXA2

Ligand	Region	MolDock Score (kcal/mol)	Interacting Residues
Lauric acid	1	-99,42	Arg179
	2	-84,21	Asn65, Arg68, Ser296
Myristic acid	1	-94,63	Asn65, Arg68
	2	-88,14	Ser22, Lys302
Palmitic acid	1	-93,35	Asp187, His224, Lys227
	2	-99,54	Asn65
Oleic acid	1	-111,42	Arg178
	2	-97,39	Ala29
Linoleic acid	1	-105,94	Arg179
	2	-112,26	Asn65, Arg68, Ser296

Preprints (www.preprints.org) | NOT PEER-REVIEWED | Posted: 18 May 2023 doi:10.20944/preprints202305.1351.v1

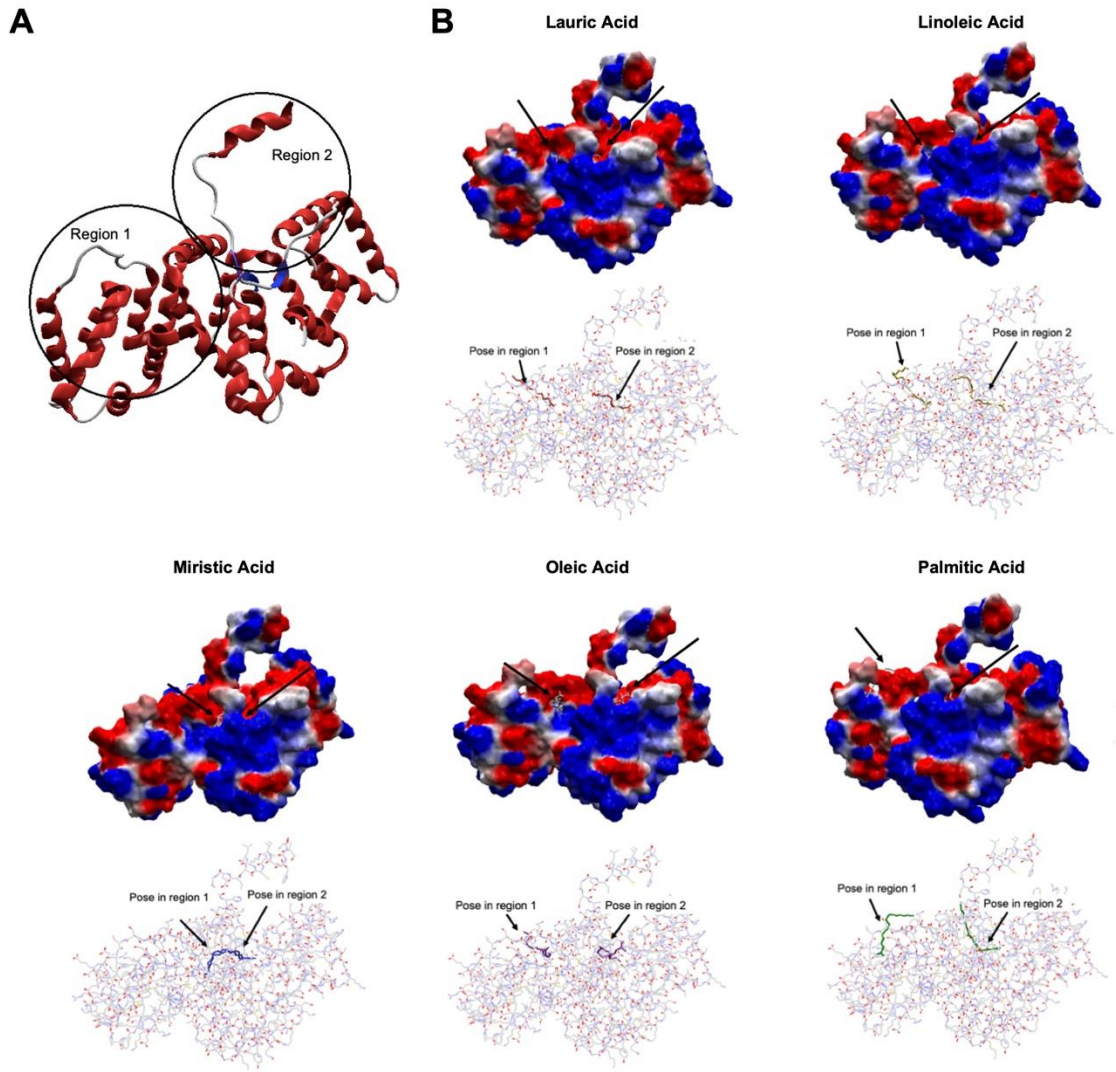

Figure 5. ANXA2 molecular docking analysis with fatty acids (**A**) Preferential regions of ANXA2 for the binding of the fatty acids: palmitic, myristic, lauric, oleic and linoleic, according to the blind docking. (**B**) Poses selected by docking for the MD simulations. ANXA2 is represented in both electrostatic surface (right) and in wire (left) representation. The arrows point the positions of the poses in regions 1 and 2.

3.6. Molecular dynamics simulations

Each of the poses illustrated in Figure 5 was submitted to steps of MD simulations, as described in the methodology, in order to evaluate its dynamic behavior and stability in the respective binding pockets over time. Pre-analysis of the results showed that the poses of region 2 presented a more stable dynamic behavior than the poses in region 1 (data no shown). This result associated to the literature finding that region 2 is important for the binding between ANXA2 and S100A10 [61-63], prompted us to focus our analysis only on the dynamics results on region 2.

Figure 6A shows the plots of total energy (average and standard deviation) of the complexes ANXA2-ligand during the MD simulations. As can be seen, all complexes presented energy < -9.5 x 105 kJ.mol^{-1} and low values of standard deviation. This means that they achieved stability during the MD simulation, corroborating the docking studies.

The values of RMSD for the complexes ANXA2-ligand are shown in Figures 6B and C. As expected, due to its larger size and mobility ANXA2 presented RMSD values higher than the ligand in all cases, never passing 8 Å, *versus* 3 Å for the ligands. These results suggest stabilization of the ligands inside the binding pocket. The higher average value of RMSD observed for the complex ANXA2-linoleic acid (Figure 6C) point to this ligand as

Preprints (www.preprints.org) | NOT PEER-REVIEWED | Posted: 18 May 2023 doi:10.20944/preprints202305.1351.v1

the less promising as binder to the region 2 of ANXA2, compared to the others, while the acids myristic and palmitic sounds like the most promising.

The plots of H-bonds formed between the ligands and ANXA2 during the MD simulations (Figure 6D) show that no ligand was capable forming more than 3 residues during the simulated time. This was already expected once the ligands are fatty acids and, therefore, bring only the carbonyl group in their structures capable of forming H-bonds. The best results were observed for the lauric and palmitic acids which formed up to 3 H-bonds with residues Asn65 and Arg68 during the whole MD simulation. The third best was myristic acid, which formed H-bonds with Lys266 and Lys322 during most of the simulation, and the worst results were of linoleic and oleic acids, which were not capable of maintaining H-bonds during most of the simulation time.

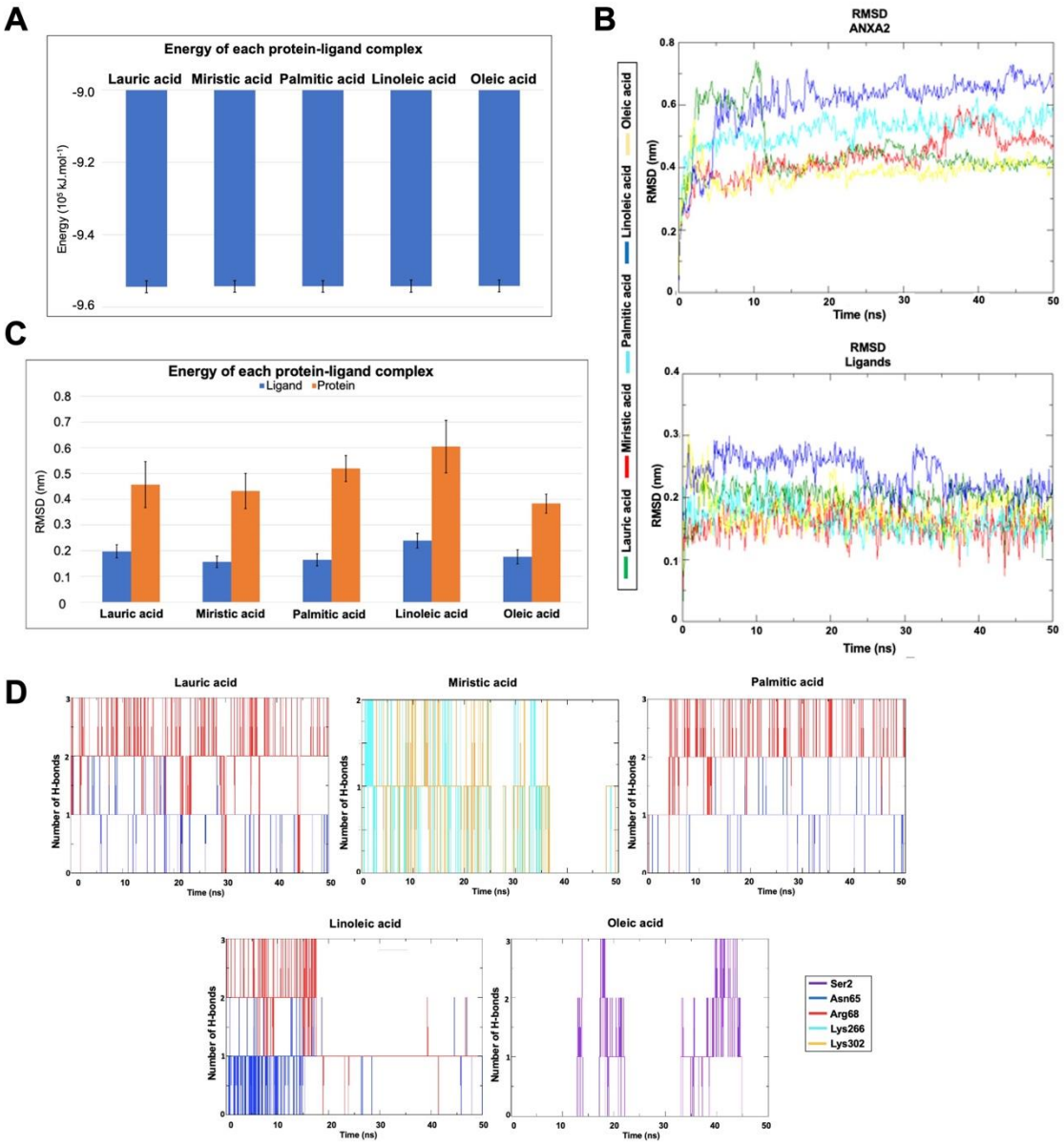

Figure 6. Molecular dynamic simulations of ANXA2 docking (**A**) Average and standard deviation of the total energy of the ANXA2-ligand complexes during the MD simulations. (**B**) RMSD plot for the complexes ANXA2-ligand during the 50 ns of MD simulation. (**C**) Average and standard deviation of RMSD for the complexes ANXA2-ligand during the MD simulations. (**D**) H-bonds observed between ANXA2 and the ligands during the MD simulation.

4. Discussion

 doi:10.20944/preprints202305.1351.v1

The main flavonoids found in açaí were quercetin, orientin and their derivatives, as well as proanthocyanidins [4,64,65]. Orientin, homoorientin, vitexin, luteolin, cryoseriol, quercetin and dihydrokaempferol have also been identified in açaí fruits [4,66].

This is the first report of the presence of nobiletin and genistein-8-C-glycoside in açaí (*Euterpe oleracea* Mart.).

In relation to açaí seed oil, the main fatty acids were: myristic acid, palmitic acid, oleic acid, linoleic acid and lauric acid. Our results show that the fixed oil extracted from the açaí seed is composed of 49.27% of saturated fatty acids and 50.73% of unsaturated fatty acids, being 29.73% monounsaturated and 20.85% polyunsaturated. Mantovani, Fernandes and Menezes (2003) described a predominance of unsaturated fatty acids, mainly oleic acid with 45.1%; 45.7%; 45.5% for pericarp, endocarp and whole fruit, respectively, followed by palmitoleic acid to a lesser extent (4.2%; 4.8%; 4.3% for pericarp, endocarp and whole fruit, making up more than 50% of the total fatty acids) [8]. ɣ-linolenic acid, linoleic acid, palmitic acid and oleic acid were the main constituents described by Mulabagal and Calderón (2012) [67]. Similar results were described by Yuyama et al. (2011) [68] and Nascimento et al. (2008) [69].

Açaí seed oil induced apoptosis and morphological changes in the CACO-2 and HCT-116 strains. To investigate the mechanisms associated with cell death, the cells were pre-treated with NAC, with an increase in cell viability. Monge-Fuentes et al. (2017), using açaí oil in nanoemulsion, found phototoxicity in melanoma cells, with reduced cell viability after treatment. In addition, the morphology of B16F10 cells showed loss of cell volume, presence of apoptotic bodies and loss of cell adhesion [34]. In the Annexin V and PI assay, cell death occurred by late apoptosis/necrosis, suggesting a photosensitizing effect with reduced proliferation of melanoma cells.

Essential oil of *Myrica gale* L., a plant native to Canada used in traditional medicine, has strong cytotoxic effects on human lung (A549) and colon (DLD-1) cancer cell lines [70] and the essential oil of *Ocimum basilicum* L. and *Psidium guajava* L., Thai medicinal plants, inhibit the proliferation of murine leukemia (P388) and oral squamous cell carcinoma cell lines, respectively [71]. Furthermore, a recent study demonstrates that pine essential oil inhibits growth and induces apoptosis in human liver carcinoma cells by down-regulating Bcl-2 expression and telomerase activity [72]. Treatment of YD-8 cells (oral cancer) with essential oil from *P. densiflora* leaves strongly inhibited proliferation and survival and induced apoptosis. Treatment with led to the generation of ROS, activation of caspase-9, cleavage of PARP, downregulation of Bcl-2 and phosphorylation of ERK-1/2 and JNK-1/2 in YD-8 cells [73].

Açaí oil contains 3.4 times more phenolic acid and 2-14 times less monomeric and dimeric flavanol compared to pulp extract. Furthermore, both the extract and the oil promoted an increase in the production of reactive oxygen species (ROS) at low concentrations [74]. Marques et al. (2017) studied açaí oil and different human cells, evaluating the cytotoxicity, genotoxicity and antigenotoxicity of *Euterpe oleracea*. For the study, HepG2 cells (hepatoma) and human leukocytes were used. There was no cytotoxic effect in the strains used [27].

Finally, Dias et al. (2014) evaluated the potential pro-apoptotic effect of açaí-derived polyphenols on HT-29 and SW-480 colorectal adenocarcinoma cells. The results showed that the açaí polyphenolic extract at concentrations from 5 to 20 mg/L) inhibited the growth of SW-480 and HT-29 cells, with greater reductions for SW-480 cells, also reducing the production of reactive species of oxygen (ROS) [33].

There was an increase in the expression of LC3-B in cells treated with seed oil and a reduction in the expression of LC3-B when pre-treated with NAC. In the evaluation of annexin expression in cells treated with açaí seed oil, the bands under the annexin were indicative of apoptosis. The cell cleaves ANXA2 forming a truncated shape. The CACO-2 strain showed more isoforms, which corroborated the annexin apoptosis assay.

Autophagy is a process of autodigestion aimed at recycling damaged cellular components and organelles in response to various stressful conditions [75]. In tumor cells, autophagy plays dual roles in tumor promotion and suppression [76].

 doi:10.20944/preprints202305.1351.v1

The close interaction between ROS and autophagy is reflected in 2 ways: the induction of autophagy by oxidative stress and the reduction of ROS by autophagy [77].

Induction of autophagy after nutrient starvation requires the production of hydrogen peroxide that oxidizes autophagy-related protein (ATG) 4. Of the ATG proteins, ATG4 is the only protease that regulates autophagy by processing and deconjugating ATG8 [78]. The oxidation modification mainly inactivates the delipidating activity of ATG4, leading to increased formation of autophagosomes associated with light chain 3 [79,80].

In addition to the above, which is considered a direct mechanism, an indirect induction of autophagy by ROS can also occur. Adenosine monophosphate (AMP)-activated protein kinase (AMPK), which can suppress the activity of the mammalian target of rapamycin (mTOR), is activated by ROS and leads to the induction of autophagy [81].

Annexin A2 is overexpressed in clear cell renal carcinoma, breast, cervical, colorectal, endometrial, hepatocellular carcinoma, lung cancer, ovarian cancer, pancreatic duct adenocarcinoma, glioblastoma, urothelial carcinoma, acute lymphoblastic leukemia, acute promyelocytic leukemia and multiple myeloma [82-93].

Regarding molecular docking and molecular dynamics, the five fatty acids studied presented theoretical results that suggest the formation of stable complexes with ANXA2. Additionally, these acids bind preferentially to the region close to the N-terminal moiety of this protein where the complexation with S100A10, which is suspected of triggering the growing and proliferation of cancer cells, occurs. Therefore, our results suggest that these acids have the potential of impairing the formation of the ANXA2-S100A10 complex, contributing for the interruption or slowing of the proliferation of cancer cells.

In studies that investigated Annexin A2 using immunohistochemistry, high expression of Annexin A2 was significantly correlated with tumor size, poorly differentiated tumors, depth of invasion and TNM stage in colorectal cancer [93]. Annexin A2 has been shown to be an independent factor of poor prognosis in patients with colorectal cancer [94]. Annexin A2 in the cell membrane is a hallmark of highly invasive tumors. This ability to invade tissue shows how Annexin A2 can affect lymph node metastasis [84,88]. Annexin A2 has also been shown to be important for the effect of progastrins and gastrins, partially mediating the effect of growth factors on colon cancer cells [95].

Annexin collaborates with different proteins such as plasminogen, S100A10 and HE4. It may be the complex interaction between these agents and Annexin A2 that plays a role in their malignant potential. Activation by phosphorylation appears to play a role in carcinogenesis and to some extent Annexin A2 appears to be regulated by Annexin A5. This accentuates the need to investigate the expression patterns of different annexins within different forms of cancer. The ongoing regulation and collaboration of Annexin A2 could be the basis for its malignant potential and could be the focus for further investigation into targeting treatment for annexins and plasminogen, S100 and HE4 proteins [61].

Thus, the *in vitro* effects of açaí seed oil in decreasing annexin expression in colorectal adenocarcinoma cells and the result of molecular docking suggest a promising effect of this natural product in modulating the regulation of annexin and, therefore, decreasing its effects. proliferative at the cellular level.

5. Conclusions

Considering the results obtained so far, the açaí seed oil is a promising phytochemical product for the development of drug-active compounds with antitumor effect. The use of seed, a product that is usually discarded, will also contribute to sustainable development and to stimulate the green economy of traditional communities, especially in the North and Northeast regions.

Author's contributions: Conceptualization: M.A.C.N.S, K.R.A.B; M.R.R; Data curation, Investigation, Methodology: M.A.C.N.S; J.W.T., L.A.S.W, K.R.A.B, M.R.R, F.D.B, L.A.V., T.C.C.F, J.A.M.D. Supervision: M.C.L.B, M.D.S.B.N and J.E.C. Writing – original draft: M.A.C.N.S, J.W.T and M.R.R; Writing – review and editing: M.A.C.N.S, M.R.R, M.D.S.B.N and J.E.C. All authors have read and agreed to the published version of the manuscript.

Funding: This work was supported by Fundação de Amparo à Pesquisa e ao Desenvolvimento Científico e Tecnológico do Estado do Maranhão (FAPEMA) – Notice 002/2019 Universal

Institutional Review Board Statement: Not applicable.

Informed Consent Statement: Not applicable.

Ethical Statement: Not applicable

Acknowledgments: We would like to thank you to Nucleum of Basic and Applied Immunology from Federal University of Maranhão, to Cell Structure and Dynamics Group, Cellular and Molecular Oncobiology Program, National Cancer Institute and to Laboratory of Molecular Modeling Applied to Chemical and Biological Defense (LMCBD), Military Institute of Engineering for providing research activities.

Competing interests: There are no conflicts of interest in this research.

Data availability statement: All data is included in the manuscript.

References

1. Sung, H., Ferlay, J., Siegel, R.L., Laversanne, M., Soerjomataram, I., Jemal, A., et al., 2021. Global Cancer Statistics 2020: GLOBOCAN Estimates of Incidence and Mortality Worldwide for 36 Cancers in 185 Countries. CA Cancer J Clin. 2021 May;71(3):209-249. https://doi.org/10.3322/caac.21660
2. Brasil. Instituto Nacional de Câncer José Alencar Gomes da Silva, 2022. Estimativa 2023: incidência de câncer no Brasil / Instituto Nacional de Câncer Rio de Janeiro: Inca, 2022.
3. Empresa Brasileira de Pesquisa Agropecuária (Embrapa). Sistema De Produção Do Açaí, 2006 Available in: <http://sistemasdeproducao.cnptia.embrapa.br/FontesHTML/Acai/SistemaProducaoAcai_2ed/index.htm> Access in 08 aug. 2018.
4. Gallori, S., Bilia, A.R., Bergonzi, M.C., Barbosa, W.L.R., Vincieri, S.S., 2004. Polyphenolic constituents of anthocyanins from the açaí fruit (*Euterpe oleracea*) Mart. Cienc. Tecnol. Aliment. 20, 388–390. https://doi.org/10.1365/s10337-004-0305-x.
5. Rodrigues, R.B., Lichtenthäler, R., Zimmermann, B.F., Papagiannnopoulos, M., Fabricius, H., Marx, F., et al., 2006. Total oxidant scavenging capacity of *Euterpe oleracea Mart*. (açaí) seeds and identification of their polyphenolic compounds. J Agric Food Chem. 54, 4162–7. https://doi.org/10.1021/jf058169p
6. Schauss, A.G., Wu, X., Prior, R.L., Ou, B., Patel, D., Huang, D., Kababick J.P., 2006. Phytochemical and nutrient composition of the freeze-dried amazonian palm berry, *Euterpe Oleraceae* Mart. (Açaí). J Agric Food Chem. 54 (22), 8598-603. https://doi.org/10.1021/jf060976g
7. Chin, Y.W., Chai, H.B., Keller, W.J., Kinghorn, D., 2008. Lignans and other constituents of the fruits of *Euterpe oleracea* (Açaí) with antioxidant and cytoprotective activities. J. Agric. Food Chem**,** 56, 7759–7764. https://doi.org/10.1021/jf801792n.
8. Mantovani, I.S.B., Fernandes, S.B.O., Menezes, F.S., 2003 et al. Constituintes apolares do fruto do açaí (*Euterpe oleracea* M. - *Arecaceae*). Rev. Bras. Farmacogn. 13 (1), 41-2. https://doi.org/10.1590/S0102-695X2003000300016
9. Oliveira, M.S.P., Carvalho, J.E.U., Nascimento, W.M.O., Müller, C.H., 2002 Cultivo do açaizeiro para produção de frutos. Belém: EMBRAPA-CPATU. (Circular Técnica, 26).
10. Mourão, L., 2010. História e natureza: do açaí ao palmito. Rev Territórios e Fronteiras, 3(2): 74-96. https://doi.org/10.22228/rtf.v3i2.69
11. Lee, R., Balick, M.J., 2008. Palms, people, and health. Explore. 4 (1): 59–62. https://doi.org/10.1016/j.explore.2007.10.009
12. Goulding, M., Smith, N., 2007. Palms. Sentinels for Amazon Conservation. Amazon Conservation Association & Missouri Botanical Garden, St. Louis, MO, USA, p. 356.
13. Henderson, A.,1995. The Palms of the Amazon, University Press: Oxford
14. Brian, M.B., 1988. Etnobotany of the Chacobo Indians and their Palms Advanced in Economic Botany, The New York Botanic Garden: New York.
15. Prance, G.H., Silva, M.F., 1975. Árvores de Manaus, INPA: Manaus, 312p
16. Kahn, F., Granville, J., 1992. Palms in Forest Ecosystems of Amazonia, Ecological Studies no. 95, Spring Verlag: New York.
17. Marinho, B.G., Herdy, S.A., Sá, A.C., Santos, G.B., Matheus, M.E., Menezes, F.S., Fernandes, P.D., 2002. Atividade antinociceptiva de extratos de açaí (*Euterpe oleracea* Mart.). Rev. Bras. Farmacogn. 12:52–53. https://doi.org/10.1590/S0102-695X2002000300025
18. Heitor, R. da S., Daniele, da C. de A., Ariadna, L. P., Hady, K., Jesus, R. R. A., & José, C. T. C., 2017. Euterpe oleracea Mart. (açaí): an old known plant with a new perspective. African Journal of Pharmacy and Pharmacology. 10(46): 995–1006. https://doi.org/10.5897/ajpp2016.4686
19. Peixoto, H., Roxo, M., Krstin, S., Wang, X., Wink, M., 2016. Anthocyanin-rich extract of açaí (Euterpe precatoria Mart.) mediates neuroprotective activities in Caenorhabditis elegans. Journal of Functional Foods. 26:385-393. 10.1016/J.JFF.2016.08.012
20. Romualdo, G.R., Fragoso, M.F., Borguini, R.G., de Araújo Santiago, M.C.P., Fernandes, A.A.H., Barbisan, L.F., 2015. Protective effects of spray-dried açaí (Euterpe oleracea Mart) fruit pulp against initiation step of colon carcinogenesis. Food Res Int, 77: 432-440. 10.1016/J.FOODRES.2015.08.037

21. Torma, P. do C.M.R., Brasil, A.V.S., Carvalho, A.V., Jablonski, A., Rabelo, T. K., Moreira, J. C. F. Rios, A.de O., 2017. Hydroethanolic extracts from different genotypes of açaí (Euterpe oleracea) presented antioxidant potential and protected human neuron-like cells (SH-SY5Y). Food Chem. 222:94–104. https://doi.org/10.1016/J.FOODCHEM.2016.12.006.
22. Yamaguchi, K. K. de L., Pereira, L.F.R., Lamarão, C.V., Lima, E.S., da Veiga-Junior, V.F., 2015. Amazon açaí: Chemistry and biological activities: A review. Food Chem. 179:137–151.https://doi.org/10.1016/J.FOODCHEM.2015.01.055.
23. Melhorança Filho, A.L., Pereira, M.R.R., 2012. Atividade antimicrobiana de óleos extraídos de açaí e de pupunha sobre o desenvolvimento de *Pseudomonas aeruginosa* e *Staphylococcus aureus*. Biosci. J. 28: 598–603
24. Magalhães, T.S.S.D.A., Macedo, P.C.D.O., Pacheco, S.Y.K., Silva, S.S., da Barbosa, E.G., Pereira, R.R., Costa, R.M.R., Junior, J.O.C.S., Ferreira, M.A.D.S., Almeida, J.C.D., et al., 2020. Development and evaluation of antimicrobial and modulatory activity of inclusion complex of *Euterpe oleracea* Mart oil and β-cyclodextrin or hp-β–cyclodextrin. Int. J. Mol. Sci. 21:e942. https://doi.org/10.3390/ijms21030942
25. Favacho, H.A.S., Oliveira, B.R., Santos, K.C., Medeiros, B.J.L., Sousa, P.J.C., Perazzo, F.F., Carvalho, J.C.T., 2011. Anti-inflammatory and antinociceptive activities of *Euterpe oleracea* oil. Braz. J. Pharmacogn. 21:105–114. https://doi.org/10.1590/S0102-695X2011005000007
26. Souza, B.S.F., Carvalho, H.O., Ferreira, I.M., da Cunha, E.L., Barros, A.S., Taglialegna, T., Carvalho, J.C.T., 2017. Effect of the treatment with *Euterpe oleracea* Mart. oil in rats with Triton-induced dyslipidemia. Biomed. Pharm. 90: 542–547. https://doi.org/10.1016/j.biopha.2017.04.005
27. Marques, E.S., Tsuboy, M.S.F., Carvalho, J.C.T., Rosa, P.C.P., Perazzo, F.F., Gaivão, I.O.M., Maistro, E.L., 2017. First cytotoxic, genotoxic, and antigenotoxic assessment of Euterpe oleracea fruit oil (açaí) in cultured human cells. Genet Mol Res. 17:16(3). https://doi.org/10.4238/gmr16039700
28. Stoner, G.D., Wang, L.S., Seguin, C., Rocha, C., Stoner K., Chiu, S., Kinghorn A.D., 2010. Multiple berry types prevent N-nitrosomethylbenzylamine- induced esophageal cancer in rats. Pharm Res. 27, 6, 1138-45. https://doi.org/10.1007/s11095-010-0102-1.
29. Fragoso, M.F., Prado, M.G., Barbosa, L., Rocha, N.S., Barbisan, L.F., 2012. Inhibition of mouse urinary bladder carcinogenesis by açaí fruit (*Euterpe oleraceae* Martius) intake. Plant Foods Hum Nutr. 67 (3), p235-41. https://doi.org/10.1007/s11130-012-0308-y
30. Fragoso, M.F., Romualdo, G.R., Ribeiro, D.A., Barbisa, L.F., 2013 et al. Açaí (*Euterpe oleracea* Mart.) feeding attenuates dimethylhydrazine-induced rat colon carcinogenesis. Food Chem Toxicol. 58, 68-76. https://doi.org/10.1016/j.fct.2013.04.011
31. Fragoso, M.F., Romualo, G.R., Vanderveer, L.A., Franc-Barraza, J., Cukierman, E., Clapper, M.L., Carvalho, R.F., Barbisan, L.F., 2018. Lyophilized açaí pulp (*Euterpe oleracea* Mart) attenuates colitis-associated colon carcinogenesis while its main anthocyanin has the potential to affect the motility of colon cancer cells. Food Chem Toxicol. Sep 6, 121, 237-245. https://doi.org/10.1016/j.fct.2018.08.07
32. Choi, Y.J., Choi, Y.J., Kim, N., Nan, R.H., Lee, S., Lee, H.S., Lee, H.N., Surh, Y.J., Lee, D.H., 2017. Açaí berries inhibit colon tumorigenesis in azoxymethane/dextran sulfate sodium-treated mice. Gut Liver. 11 (2), p. 243-52. https://doi.org/10.5009/gnl16068
33. Dias, M.M.D.S., Noratto, G., Martino, H.S.D., Arbizu, S., Peluzio, M.C.G., Talcott, S., Ramos, A.M., Mertens-Talcott, S.U., 2014. Pro-apoptotic activities of polyphenolics from açai (*Euterpe oleracea* Martius) in human SW-480 colon cancer cells. Nutr. Cancer. 66:1394–1405. https://doi.org/10.1080/01635581.2014.956252
34. Monge-Fuentes, V., Muehlmann, L.A., Longo, J.P.F., Silva, J.R., Fascineli, M.L., de Souza, P., et al., 2017. Photodynamic therapy mediated by açaí oil (*Euterpe oleracea* Martius) in nanoemulsion: A potential treatment for melanoma. J Photochem Photobiol. 166, 301-10. https://doi.org/10.1016/j.jphotobiol.2016.12.002
35. Alessandra-Perini, J., Alessandra-Perini, J., Rodrigues-Baptista, K.C., Soares de Moura, R., Palumbo Júnior, A., dos Santos, T.A., et al., 2018. *Euterpe oleracea* extract inhibits tumorigenesis effect of the chemical carcinogen DMBA in breast experimental cancer. BMC Complement Altern Med. 2(18), p.116. https://doi.org/10.1186/s12906-018-2183-z
36. Silva, D.F., Vidal, F.C.B., Santos, D., Costa, M.C.P.C., Morgado-Díaz, J.A., Nascimento, M.D.S.B.N, Moura, R.S., 2014. Cytotoxic effects of *Euterpe oleracea* Mart. in malignant cell lines. BMC Complement Altern Med. 14, 175. https://doi.org/10.1186/1472-6882-14-175
37. Silva, M.A.C.N., Costa, J.H., Pacheco-Fill, T., Ruiz, A.L.T.G., Vidal, F.C.B., Borges, K.R.A, et al., 2021. Açai (*Euterpe oleracea* Mart.) Seed Extract Induces ROS Production and Cell Death in MCF-7 Breast Cancer Cell Line. Molecules. Jun 10;26(12):3546. https://doi.org/10.3390/molecules26123546
38. Freitas, D.D.S., Morgado-Díaz, J.A., Gehren, A.S., Vidal, F.C.B., Fernandes, R.M.T., Romão, W., et al., 2017. Cytotoxic analysis and chemical characterization of fractions of the hydroalcoholic extract of the *Euterpe oleracea* Mart. seed in the MCF-7 cell line. J Pharm Pharmacol. 69(6),714-21. https://doi.org/10.1111/jphp.12679
39. Chiang, Y., Rizzino, A., Sibenaller, Z.A., Wold, M.S., Vishwanatha, J.K., 1999. Specific down-regulation of annexin II expression in human cells interferes with cell proliferation. Mol Cell Biochem. Sep;199(1-2):139-47. https://doi.org/10.1023/A:100694212867
40. Soares de Moura, R., Costa, G.F., Moreira, A.S.B., Queiroz, E.F., Moreira, D.D.C., Garcia-Souza, E.P., et al., 2012. Vitis vinifera L. grape skin extract activates the insulin-signalling cascade and reduces hyperglycaemia in alloxan- induced diabetic mice. J Pharm Pharmacol.Feb;64(2):268-76. https://doi.org/10.1111/j.2042-7158.2011.01395.x
41. 41. Hartman, L., Lago R.C., 1973. Rapid preparation of fatty acid methyl esters from lipids. Lab Pract. Jul;22(6):475-6
42. Albuquerque-Xavier, A.C., Bastos, L.G.R., Freitas Jr, J.C.M., Leve, F., de Souza, W.F., Araujo, W.M., et al., 2012. Blockade of irradiation-induced autophagosome formation impairs proliferation but does not enhance cell death in HCT-116 human colorectal carcinoma cells. Int J Oncol, 40 (4), p-1267-76. https://doi.org/10.3892/ijo.2012.1329

43. Shao, C., Zhang, F., Kemp, M.M., Linhardt, R.J., Waisman, D.M., Head, J.H., Seaton, B.A., 2006. Crystallographic Analysis of Calcium-dependent Heparin Binding to Annexin A2. Journal of Biological Chemistry, 281(42), p. 31689–31695. https://doi.org/10.1074/jbc.M604502200
44. Hehre, W.J., Deppmeier, B.J., Klunzinger, P.E., 1999. PC Spartan Pro molecular modeling for desktop. Chem. Eng. News. 77(17), p. 2.
45. Reed, A.E., Weinstock, R.B., Weinhold, F., 1985. Natural population analysis. J. Chem. Phys. 83(2):735–746. https://doi.org/10.1063/1.449486
46. Stewart, J.J.P., 2004. Optimization of parameters for semiempirical methods IV: Extension of MNDO, AM1 and PM3 to more main group elements. J Mol Model. 10(2):155–164. https://doi.org/10.1007/s00894-004-0183-z
47. De Almeida, J.S.F.F., Cacalcante, S.F.d.A., Dolezal, R., Kuca, K., Musilek, K., Jun, D., Franca, T.C.C., 2019. Surface screening, molecular modeling and in vitro studies on the interactions of aflatoxin M1 and human enzymes acetyl- and butyrylcholinesterase. Chem Biol Interact. 308:113-119. https://doi.org/10.1016/j.cbi.2019.05.022
48. Botelho, F.D., dos Santos, M.C., Gonçalves, A.d.S., Kuca, K., Valis, M., LaPlante, S.R., França, T.C.C., de Almeida, J.S.F.D., 2020. Ligand-Based Virtual Screening, Molecular Docking, Molecular Dynamics, and MM-PBSA Calculations towards the Identification of Potential Novel Ricin Inhibitors. Toxins (Basel). 12(12):746. https://doi.org/10.3390/toxins12120746
49. Botelho, F.D., Santos, M.C., Gonçalves, A.S., França, T.C.C., LaPlante, S.R., de Almeida, J.S.F.D 2022. Identification of novel potential ricin inhibitors by virtual screening, molecular docking, molecular dynamics and MM-PBSA calculations: a drug repurposing approach. J Biomol Struct Dyn. 40(12):5309-5319. https://doi.org/10.1080/07391102.2020.1870154
50. Abraham, M.J., Murtola, T., Schulz, R., Páll, S., Smith, J.C., Hess, B., Lindahl, E., 2015. SoftwareX. 1-2:19-25. https://doi.org/10.1016/j.softx.2015.06.001
51. 51. Pronk, S.,Páll, S., Schulz, R., Larsson, P., Bjelkmar, P., Apostolov, R., Shirts, M.R., et al., 2013. GROMACS 4.5: A high-throughput and highly parallel open source molecular simulation toolkit. Bioinformatics. 29(7): 845–854. https://doi.org/10.1093/bioinformatics/btt055
52. Jorgensen, W.L., Maxwell, D.S., Tirado-Rives, J., 1996. Development and testing of the OPLS all-atom force field on conformational energetics and properties of organic liquids. J. Am. Chem. Soc. 118(45):11225–11236. https://doi.org/10.1021/ja9621760
53. Kaminski, G.A., Friesner, R.A., Tirado-Rives, J., Jorgensen, W.L., 2001. Evaluation and reparametrization of the OPLS-AA force field for proteins via comparison with accurate quantum chemical calculations on peptides. J. Phys. Chem B. 105(28):6474–6487. https://doi.org/10.1021/jp003919d
54. Sousa da Silva, A.W., Vranken, W.F., 2012. ACPYPE - AnteChamber PYthon Parser interfacE. BMC Res Notes 5(367):1-8. https://doi.org/10.1186/1756-0500-5-367.
55. Jorgensen, W.L., Chandrasekhar, J., Madura, J.D., 1983. Comparison of simple potential functions for simulating liquid water. J. Chem. Phys. 79(2):926–935. https://doi.org/10.1063/1.445869
56. Bussi, G., Donadio, D., Parrinello, M., 2007. Canonical sampling through velocity rescaling. J. Chem. Phys. 126, 014101. https://doi.org/10.1063/1.2408420
57. Parrinello, M., Rahman, A., 1981. Polymorphic transitions in single crystals: A new molecular dynamics method. Journal of Applied Physics. 52(12):7182–7190. https://doi.org/10.1063/1.328693
58. Turner, P.J., 2005. XMGRACE, Version 5.1.25. Beaverton, ORCenter for Coastal and Land-Margin Research, Oregon Graduate Institute of Science and Technology.
59. Humphrey, W., Dalke, A., Schulten, K., 1996. VMD: Visual Molecular Dynamics. J Mol Graph. 14(1):33–8, 27-8. https://doi.org/10.1016/0263-7855(96)00018-5.
60. Barth S., Glick, D., Macleod, K.F., 2010. Autophagy: assays and artfacts. J Pathol. 221(2): 117-24. https://doi.org/10.1002/path.2694
61. Bharadwaj, A., Bydoun, M., Holloway, R., Waisman, D., 2013. Annexin A2 heterotetramer: Structure and function. Int J Mol Sci. Mar 19;14(3):6259-305. https://doi.org/10.3390/ijms14036259.
62. Christensen, M.V., Hogdall, C.K., Jochumsen, K.M., Hogdall, E.V.S., 2018. Annexin A2 and cancer: A systematic review. Int J Oncol. 52(1): 5–18. https://doi.org/10.3892/ijo.2017.4197
63. Madureira, P.A., O'Connell, P.A., Surette, A.P., Miller, V.A., Waisman, D.M., 2012. The biochemistry and regulation of S100A10: A multifunctional plasminogen receptor involved in oncogenesis. J Biomed Biotechnol 2012:353687. https://doi.org/10.1155/2012/353687.
64. Lichtenthaler, R., Rodrigues, R.B., Maia, J.G.S., Papagiannopoulos, M., Fabricius, H., Marx, F., 2005. Total antioxidant scavenging capacities of *Euterpe oleracea* Mart. (açai). Int. J. Food Sci. Nutr. 56 (1): 68–75. https://doi.org/10.1080/09637480500082082
65. Pacheco-Palencia, L.A., Duncan, C.E., Talcott, S.T., 2009. Phytochemical composition and thermal stability of two commercial açai species, *Euterpe oleracea* and *Euterpe precatoria*. Food Chem. 115:1199–1205. https://doi.org/10.1016/j.foodchem.2009.01.034
66. Heinrich, M., Dhanji, T., Casselman, I., 2011. Açai (*Euterpe oleracea* Mart.) – a phytochemical and pharmacological assessment of the species' health claims. Phytochem Lett. 4(1):10-21. https://doi.org/10.1016/j.phytol.2010.11.005
67. Mulabagal, V., Calderón, A.I., 2012. Liquid chromatography/mass spectrometry based fingerprinting analysis and mass profiling of *Euterpe oleracea* (açaí) dietary supplement raw materials. Food Chem. 134:1156–1164. https://doi.org/10.1016/j.foodchem.2012.02.123.
68. Yuyama, L.K.O., Aguiar, J.P.L., Silva Filho, D.F., Yuyama, K., Varejão, M.J., Fávaro, D.I.T., et al., 2011. Physicochemical characterization of acai juice of *Euterpe precatoria* Mart. from different Amazonian ecosystems. Acta Amaz. 41:545–552. https://doi.org/10.1590/S0044-59672011000400011.

69. Nascimento, R.J.S., Couri, S., Antoniassi, R., 2008. Composição em ácidos graxos do óleo da polpa de açaí extraído com enzimas e com hexano. Rev Bras Frutic 30(2): 498–502. https://doi.org/10.1590/S0100-29452008000200040
70. Sylvestre, M., Legault, J., Dufour, D., Pichette, A., 2005. Chemical composition and anticancer activity of leaf essential oil of *Myrica gale L*. Phytomedicine.12: 299-304. https://doi.org/10.1016/j.phymed.2003.12.004
71. Manosroi, J., Dhumtanom, P., Manosroi, A., 2006. Anti-proliferative activity of essential oil extracted from Thai medicinal plants on KB and P388 cell lines. Cancer Lett. 235(1):114-120. https://doi.org/10.1016/j.canlet.2005.04.021
72. Wei, F.X., Li, M.Y., Song, Y.H., Li., H.Z., 2008. Apoptosis and activity changes of telomerase induced by essential oil from pine needles in HepG2 cell line. Zhong Yao Cai. 31(8):1197-1200.
73. Jo, J.R., Park, J.S., Park, Y.K., Chae, Y.Z., Lee, G.H., Park, G.Y., Jang, B.C., 2012. *Pinus densiflora* leaf essential oil induces apoptosis via ROS generation and activation of caspases in YD-8 human oral cancer cells. Int J Oncol. 40(4): 1238-1245. https://doi.org/10.3892/ijo.2011.1263
74. Pacheco-Palencia, L.A., Mertens-Talcott, S., Talcott, S.T., 2008. Chemical composition, antioxidant properties, and thermal stability of a phytochemical enriched oil from Açaí (*Euterpe oleracea* Mart.). J Agric Food Chem. 56(12):4631–4636. https://doi.org/10.1021/jf800161u
75. Filomeni, G., de Zio, D., Cecconi, F., 2015. Oxidative stress and autophagy: the clash between damage and metabolic needs. Cell Death Differ. 22(3):377-388. https://doi.org/10.1038/cdd.2014.150
76. Yun, C.W., Lee, S.H., 2018. The roles of autophagy in cancer. Int J Mol Sci,19(11):3466. https://doi.org/10.3390/ijms19113466
77. Li, L., Tan, J., Miao, Y., Lei, P., Zhang, Q., 2015. ROS and autophagy: interactions and molecular regulatory mechanisms. Cell Mol Neurobiol, 35:615-621. https://doi.org/10.1007/s10571-015-0166-x
78. Maruyama,T., Noda, N.N., 2017. Autophagy-regulating protease Atg4: structure, function, regulation and inhibition. J Antibiot (Tokyo). 71:72-78. https://doi.org/10.1038/ja.2017.104
79. Scherz-Shouval, R., Shvets, E., Fass, E., Shorer, H., Gil, L., Elazar, V., 2007. Reactive oxygen species are essential for autophagy and specifically regulate the activity of Atg4. EMBO J. 26:1749-1760. https://doi.org/10.15252/embj.2019101812
80. Poiller-Perez, L., Despouy, G., Delage-Mourroux, R., Boyer-Guittaut, M., 2015. Interplay between ROS and autophagy in cancer cells, from tumor initiation to cancer therapy. Redox Biol. 4:184-192. https://doi.org/10.1016/j.redox.2014.12.003
81. Emerling, B.M., Weinberg, F., Snyder, C., Burgess, Z., Mutlu, G.M., Viollet, B., Budinger. G.R.S., Chandel, N.S., 2009. Hypoxic activation of AMPK is dependent on mitochondrial ROS but independent of an increase in AMP/ATP ratio. Free Radic Biol Med. 46(10):1386-1391. https://doi.org/10.1016/j.freeradbiomed.2009.02.019
82. Spijkers-Hagelstein, J.A., Pinhanços, S.M., Schneider, P., Pieters, R., Stam, R.W., 2013. Src kinase-induced phosphorylation of annexin A2 mediates glucocorticoid resistance in MLL-rearranged infant acute lymphoblastic leukemia. Leukemia. 27: 1063-1071. https://doi.org/10.1038/leu.2012.372
83. Gopalakrishnapillai, A., Kolb, E.A., Dhanan, P., Mason, R.W., Napper, A., Barwe, S.P., 2015. Disruption of Annexin II/p11 interaction suppresses leukemia cell Binding, homing and engraftment, and sensitizes the leukemia cells to chemotherapy. PLoS One 10(10): e0140564, 2015. https://doi.org/10.1371/journal.pone.0140564
84. Yang, J., Cheng, T.T., Wang, L.N., Chen, W., Li, X., 2012. The expression and clinical significance of Annexin II in clear-cell renal cell carcinoma. Xi Bao Yu Fen Zi Mian Yi Xue Za Zhi. 28: 59-62.
85. Sharma, M.R., Koltowski, L., Ownbey, R.T., Tuszynski, G.P., Sharma, M.C., 2006. Angiogenesis-associated protein annexin II in breast cancer: Selective expression in invasive breast cancer and contribution to tumor invasion and progression. Exp Mol Pathol. 81:146-156. https://doi.org/10.1016/j.yexmp.2006.03.003
86. Choi, C.H., Chung, J.Y., Chung, E.J., Sears, J.D., Lee, J.W., Bae, D.S., Hewitt, S.M., 2016. Prognostic significance of annexin A2 and annexin A4 expression in patients with cervical cancer. BMC Cancer. 16: 448. https://doi.org/10.1186/s12885-016-2459-y
87. Xiu, D., Liu, L., Qiao, F., Yang, H., Cui, L., Liu, G., 2016. Annexin A2 coordinates STAT3 to regulate the invasion and migration of colorectal cancer cells in vitro. Gastroenterol Res Pract, 3521453, 2016. https://doi.org/10.1155/2016/3521453
88. Tristante, E., Martínez, C.M., Jiménez, S., Mora, L., Carballo, F., Martínez-Lacaci, I., Torre-Minguela, C., 2015. Association of a characteristic membrane pattern of annexin A2 with high invasiveness and nodal status in colon adenocarcinoma. Transl Res.166: 196-206. https://doi.org/10.1016/j.trsl.2015.02.006
89. Deng, L., Gao, Y., Li, X., Cai, M., Wang, H., Zhuang, H., Tan, M., Liu, S., Hao, Y., Lin, B., 2015. Expression and clinical significance of annexin A2 and human epididymis protein 4 in endometrial carcinoma. J Exp Clin Cancer Res. 34(96). https://doi.org/10.1186/s13046-015-0208-8
90. Gao, H., Yu, B., Yan, Y., Shen, J., Zhao, S., Zhu, J., Qin, W., Gao, Y., 2013. Correlation of expression levels of ANXA2, PGAM1, and CALR with glioma grade and prognosis. J Neurosurg.4(118): 846-853. https://doi.org/10.3171/2012.9.JNS112134
91. Mohammad, H.S., Kurokohchi, K., Yoneyama, H., Tokuda, M., Morishita, A., Jian G., et al., 2008. Annexin A2 expression and phosphorylation are up-regulated in hepatocellular carcinoma. Int J Oncol. 33: 1157-1163.
92. Wang, Y.X., Lv, H., Li, Z.X., Li, C., Wu, X.Y., 2012. Effect of shRNA mediated down-regulation of Annexin A2 on biological behavior of human lung adencarcinoma cells A549. Pathol Oncol Res. 18: 183-190. https://doi.org/10.1007/s12253-011-9427-2
93. Rocha, M.R., Barcellos-de-Souza, P., Sousa-Squiavinato, A.C.M., Fernandes, P.V., de Oliveira, I.M., Boroni, M., Morgado-D[iaz, J.A., 2018. Annexin A2 overexpression associates with colorectal cancer invasiveness and TGF-ß induced epithelial mesenchymal transition via Src/ANXA2/STAT3. Sci Rep. 8: 11285. https://doi.org/10.1038/s41598-018-29703-0
94. Emoto, K., Yamada, Y., Sawada, H., Fujimoto, H., Ueno, M., Takayama, T., et al., 2001. Annexin II overexpression correlates with stromal tenascin-C overexpression: A prognostic marker in colorectal carcinoma. Cancer. 92: 1419-1426. https://doi.org/10.1002/1097-0142(20010915)92:6<1419::AID-CNCR1465>3.0.CO;2-J

 doi:10.20944/preprints202305.1351.v1

95. Singh, P., Wu H., Clark, C., Owlia, A., 2007. Annexin II binds progastrin and gastrin-like peptides, and mediates growth factor effects of autocrine and exogenous gastrins on colon cancer and intestinal epithelial cells. Oncogene. 26(3): 425-44. https://doi.org/10.1038/sj.onc.1209798